Activation of C–H···Halogen (Cl, Br, and I) Hydrogen Bonds at the Organic/Inorganic Interface in Fluorinated Tetrathiafulvalenes Salts

Olivier J. Dautel,[a] Marc Fourmigué,*[a] and Enric Canadell[b]

Abstract: The electrocrystallization of fluorinated bis(2,2′-difluoropropylenedithio)tetrathiafulvalene (**1**) in the presence of linear (ICl_2^-, IBr_2^-, I_2Br^-) or cluster ($[Mo_6Cl_{14}]^{2-}$) anions affords 1:1 and 2:1 cation radical salts such as [**1**][ICl_2] and [**1**]$_2$[Mo_6Cl_{14}]·(CH_3CN)$_2$. In both salts, the **1**$^{+\cdot}$ radical ion adopts a boat conformation and envelops the anion through C–H···Hal$_{anion}$ (Hal$_{anion}$ = Cl, Br, I) hydrogen bonds. This demonstrates the activating role of the neighboring electron-withdrawing CF_2 moieties in the stabilization of bi- or trimolecular neutral entities. With smaller linear anions, fluorine segregation controls the solid-state associations of the bimolecular [**1**]$^{+\cdot}$[X]$^-$ entities, and gives rise to layered materials with a limited overlap interaction between the open-shell organic cations and magnetic spin chain behavior. With the larger $[Mo_6Cl_{14}]^{2-}$ ions, a strong overlap interaction between radical cations gives rise to diamagnetic [**1**]$_2^{2+}$ dimers, which alternate with the cluster anions to form hybrid organic/inorganic ···[**1**]$_2^{2+}$[Mo_6Cl_{14}]$^{2-}$··· chains. This behavior is also observed in [**2**]$_2^{2+}$[Mo_6Cl_{14}]$^{2-}$·(CH_2Cl_2)$_2$, in which compound **2** is the unsymmetrically substituted (ethylenedithio)(2,2′-difluoropropylenedithio)tetrathiafulvalene. On the other hand, the unsymmetrically substituted 2,2′-difluoropropylenedithiotetrathiafulvalene (**3**) affords a mixed-valence 4:1 salt with $[Mo_6Cl_{14}]^{2-}$, which is formulated as [**3**]$_4$[Mo_6Cl_{14}]·(CH_3CN)$_2$. This semiconducting salt is characterized by the coexistence of both the fluorine/fluorine segregation (with solvent inclusion) *and* the organic/inorganic segregation (with delocalized overlap interactions). Both C_{sp^2}–H···Cl and C_{sp^3}–H···Cl hydrogen bonds facilitate the stabilization of the organic/inorganic interface and the presence of conducting organic slabs.

Keywords: crystal engineering · fluorine · hydrogen bonds · magnetic properties · molecular recognition

Introduction

In order to take advantage, in the solid state, of the well-known segregation effects which are observed in fluid phases with highly fluorinated molecules,[1] we have recently studied the synthesis and electrochemical properties of a series of fluorinated tetrathiafulvalenes (TTF) **1**–**3** that bear one or two CF_2 groups on their outer ends.[2]

We have shown that the introduction of SCH_2 spacers between the fluorinated moiety and the TTF redox core preserves their π-redox donor ability despite the presence of the electron-withdrawing CF_2 groups. The neutral unoxidized molecules organize into layered solids in the solid state, with a peculiar fluorous bilayer which is stabilized by full fluorine segregation and a network of C–H···F hydrogen bonds.[3] Investigation of the crystallization of the radical cation salts from these donor molecules may help us to understand the competition between those fluorine segregation effects, which are observed in the neutral state, and the overlap interaction of the open-shell, delocalized molecules. These HOMO···HOMO overlap interactions are strong and directional, and tend to associate molecules into dimers, trimers, or extended one- or two-dimensional organic networks with delocalized electronic states, which are a prerequisite for electronic conductivity.[4] However, such salts will include counter anions in the solid that may affect these interactions with the organic part. In this paper, we describe several examples of radical cation salts of the fluorinated donor molecules **1**–**3** with halogenated anions of different size, shape, and charge such as

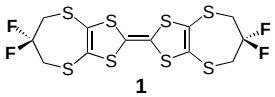

1

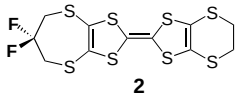

2

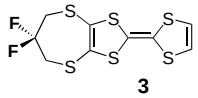

3

[a] Dr. M. Fourmigué, Dr. O. J. Dautel
Sciences Moléculaires aux Interfaces
CNRS FRE 2068 , Institut des Matériaux Jean Rouxel
2, rue de la Houssinière,
BP32229, 44322 Nantes cedex 3 (France)
Fax: (+33) 2 40 37 39 95
E-mail: fourmigue@cnrs-imn.fr

[b] Dr. E. Canadell
Institut de Ciència de Materials de Barcelona (CSIC)
Campus de la UAB, 08193 Bellaterra (Spain)

  0947-6539/01/0712-2635 $ 17.50+.50/0

the linear ICl_2^- or the anion cluster $[Mo_6Cl_{14}]^{2-}$. We analyze the competing roles of the different intermolecular interactions that stabilize the overall crystalline and electronic structure. The comparison with the layered organic conductors derived from the non-fluorinated analogues such as bis(ethylenedithio)tetrathiafulvalene (BEDT–TTF) or bis(propylenedithio)tetrathiafulvalene (BPDT–TTF) will be particularly useful. These layered conducting salts are structurally characterized by a two-dimensional organic/inorganic segregation, which is stabilized at the interface by a set of flexible, weak C–H···X (X = O, N, Hal) hydrogen bonds,[5, 6, 7] while in compounds **1**–**3** CF_2 rather than CH_2 fragments are localized at the extremities of the donor molecules.

In this respect, stronger intermolecular interactions[8] such as O–H···O or N–H···O hydrogen bonding,[9, 10] Hal···Hal[11, 12] or Hal···N[13, 14] interactions (the *halogen* bonding)[15] have been successfully faced with the HOMO···HOMO overlap interactions of properly functionalized tetrathiafulvalenes. This highlights the synergistic effects between different interactions. For example, the hydrogen-bond donor character of the NH group of tetrathiafulvalenyl amides[9] is enhanced strongly in the oxidized cationic state. Simultaneously, the hydrogen-bond acceptor character of the carbonyl function is suppressed to the advantage of the counter anion. The point we would like to address here lies in the alternative use of an aliphatic fluorine TTF functionalization whose structural effects are based on the absence of interaction; this results in the segregation of fluorinated fragments rather than in a strong and directional interaction such as hydrogen or halogen bond.

Abstract in French: *L'électrocristallisation du tétrathiafulvalène fluoré **1**, le bis(2,2'-difluoropropylènedithio)tétrathiafulvalène en présence d'anions linéaires (ICl_2^-, IBr_2^-, I_2Br^-) ou d'anions clusters ($[Mo_6Cl_{14}]^{2-}$) conduit à des sels de stoechiométrie 1:1 et 2:1 tel que **[1]**[ICl_2] et **[1]**$_2[Mo_6Cl_{14}]\cdot(CH_3CN)_2$. Dans les deux sels, le radical cation $\mathbf{1}^{\bullet+}$ adopte une forme bateau et enveloppe l'anion grâce à des liaisons hydrogène C–H···Hal_{anion} (Hal_{anion} = Cl, Br, I), démontrant ainsi l'activation des méthylènes par les CF_2 en ortho pour la stabilisation d'entités bi- ou trimoléculaires neutres. Avec les anions linéaires, la ségrégation des atomes de fluor contrôle l'organisation à l'état solide des entités bimoléculaires $[\mathbf{1}]^{\bullet+}[X]^-$ et conduit à une structure lamellaire avec un recouvrement faible entre cations radicaux et un comportement de chaîne magnétique. Avec l'anion plus gros $[Mo_6Cl_{14}]^{2-}$, un fort recouvrement entre radicaux cations conduit à des dimères diamagnétiques $[\mathbf{1}]_2^{2+}$ qui alternent avec les anions clusters au sein de chaînes mixtes organique/inorganique $\cdots[\mathbf{1}]_2^{2+}[Mo_6Cl_{14}]^{2-})\cdots$, observées aussi dans $[\mathbf{2}]_2^{\bullet+}[Mo_6Cl_{14}]^{2-}\cdot(CH_2Cl_2)_2$ avec le dérivé dissymétrique (éthylènedithio)(2,2'-propylènedithio)tétrathiafulvalène (**2**). Enfin, le (2,2'-difluoropropylènedithio)tétrathiafulvalène **3** conduit avec $[Mo_6Cl_{14}]^{2-}$ à un sel à valence mixte de stoechiométrie 4:1, $[\mathbf{3}]_4[Mo_6Cl_{14}]\cdot(CH_3CN)_2$. Ce semi-conducteur est caractérisé par la présence simultanée d'une ségrégation des atomes de fluor (avec inclusion de solvant) et d'une ségrégation organique/inorganique (avec des interactions de recouvrement étendues). Les liaisons hydrogène C_{sp^2}–H···Cl et C_{sp^3}–H···Cl stabilisent ensemble l'interface organique/inorganique et la présence des plans organiques conducteurs.*

Results and Discussion

Molecular C–H···Cl pincers of the symmetrically substituted 1: Electrocrystallization of **1** in the presence of the n-Bu_4N^+ salts of the ICl_2^-, IBr_2^-, and I_2Br^- linear ions affords three isostructural compounds of 1:1 stoichiometry, while every attempt that used the longer I_3^- ion proved unsuccessful. The salts crystallize in the orthorhombic system, space group $Cmc2_1$ and both the organic radical cation and the linear anion have a mirror plane that contains I1 and is perpendicular to the long axis of the molecules (Figure 1). The I_2Br^- ion is a

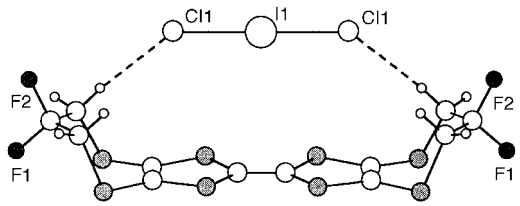

Figure 1. The bimolecular complex formed on the association of the $\mathbf{1}^{\bullet+}$ and ICl_2^- ions in [**1**][ICl_2]. The two C–H···Cl hydrogen bonds are shown as dashed lines (see Table 1).

50:50 mixture of the two non-centrosymmetrical I-I-Br^- and Br-I-I^- ions that are disordered on the mirror plane.[16] In contrast to the structure of the neutral **1**, which has a chair conformation,[2] the $\mathbf{1}^{\bullet+}$ radical ion adopts a boat conformation with one anion specifically anchored above the molecular plane through two C–H···Hal interactions. Table 1 details the geometry of the hydrogen bonds in the three salts. The short H···Hal bond lengths and a strong linearity (C–H···Hal angle $\approx 166^\circ$) compare favorably with the recently reported statistical values for C–H···Hal hydrogen bonds,[3, 17, 18] and are at the origin of the striking recognition pattern observed here. They also highlight a specific role of the CF_2 groups, whose electron-withdrawing nature activates neighboring sp^3 methylenic protons to enter into C–H···X (X = O, N, Hal) hydrogen bonds. These formally bimolecular, neutral $[\mathbf{1}]^{\bullet+}[X]^-$ moieties are arranged into layers in the solid state, shown in Figure 2. The layers are characterized by segregated

Table 1. Geometrical characteristics of the C–H···Hal (Hal = Cl, Br) hydrogen bonds that stabilize the bimolecular units in the salts of **1** with ICl_2^-, IBr_2^-, and I_2Br^- (Figure 1).

Salt	H···Hal [Å]	C···Hal [Å]	C–H···Hal [°]
[**1**][ICl_2]	2.67 (H4A···Cl1^{i})[a]	3.624(7)	166
[**1**][IBr_2]	2.69 (H4A···Br1^{i})[a]	3.643(8)	166
[**1**][I_2Br]	2.74 (H4A···Br1^{ii})[b]	3.69(1)	166

[a] Symmetry operation i: $1-x$, y, $-1-z$. [b] Symmetry operation ii: x, $1-y$, $-1/2+z$.

0947-6539/01/0712-2636 $ 17.50+.50/0 *Chem. Eur. J.* **2001**, *7*, No. 12

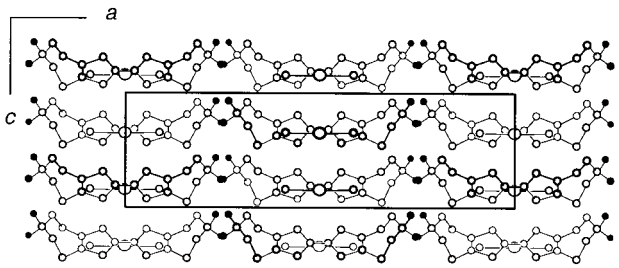

Figure 2. A view of the unit cell of [**1**][ICl_2] which shows the layered structure and the segregation of the fluorine atoms (in black).

CF_2 groups that face each other to form a fluorous bilayer which is reminiscent of that observed in the structure of the neutral **1**.[2] At this interface, short C–H···F interactions are also observed, with F···H distances of 2.5–2.6 Å and C–H···F angles between 140 and 150°. However, it is not clear whether the fluorine segregation effect is the result of the well-known tendency of fluorinated moieties to segregate or whether these bilayers are further stabilized by such C–H···F "hydrogen bonds". While Dunitz and Taylor[19] concluded from a statistical CSD (Cambridge Structural Database) survey that "organic fluorine hardly ever accept hydrogen bonds" with strong hydrogen bond donors such as *O*H or *N*H, Howard et al.[20] observed that C–H···F–C contacts were more frequently found than O/N–H···F–C ones. It was later shown[21, 22] that sp^2 hydrogen atoms of fluorinated aromatics were able to engage in C–H···F–C hydrogen bonds with short H···F distances ($< \Sigma_{\text{van der Waals}}(H,F) = 2.67$ Å) and with a preference for linearity ($140° < \text{C–H···F angle} < 180°$). The short H···F contacts identified in the interlayer space are probably weak, but could contribute to the overall stability of the layer. Their influence on the structure is confirmed here by the clear geometrical preferences revealed by a scatterplot of the C–H···F angle against the H···F distances observed in the three salts and the neutral donor molecule (Figure 3). The

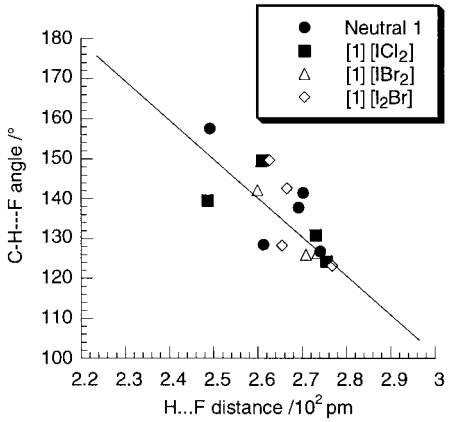

Figure 3. A scatterplot of C–H···F angles against H···F distances in neutral **1** and in its three salts with ICl_2^-, IBr_2^-, and I_2Br^-. The line represents the correlation found in fluoroaromatics.[21]

limited dispersion above and below the master line, which correlates distance and angle, compares very favorably with the similar scatterplots described by Desiraju in fluoroarenes, and contrasts with the fluorinated compounds described in the CSD.[21] Of particular note is the similarity of the structure described by Shibaeva,[23] which involves bis(thiopropylenedithio)tetrathiafulvalene (**4**), in which sulfur atoms replace the CF_2 groups of **1**. Its salt with IBr_2^- exhibits a very similar motif (Figure 4). This demonstrates that the shape of the bimolecular [**4**]$^{\bullet+}$[IBr_2]$^-$ species, which is stabilized through two C–H···Br hydrogen bonds (H···Br: 2.64 Å, C–H···Br: 152°), controls the overall solid-state arrangement rather than the fluorous bilayer structural motif alone.

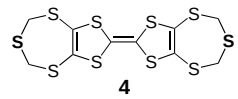

4

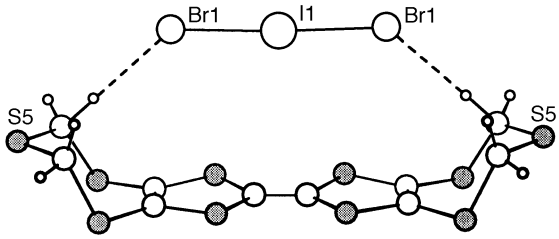

Figure 4. The bimolecular complex formed on the association of the **4**$^{\bullet+}$ and IBr_2^- ions in [**4**][IBr_2] described by Shibaeva et al.[23] The two C–H···Br hydrogen bonds are indicated as dashed lines.

Finally, if we concentrate on one single layer (Figure 5), the bimolecular [**1**]$^{\bullet+}$[ICl_2]$^-$ paramagnetic units are organized orthogonally to each other. The shortest S···S distances range from 3.600(3) Å in the ICl_2^- salt to 3.659 in the I_2Br^- salt and

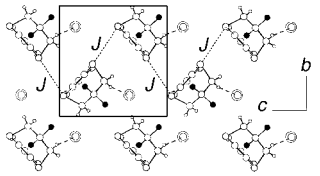

Figure 5. The mixed organic/inorganic layer, viewed along the common long axis of the **1**$^{\bullet+}$ and ICl_2^- ions. The dashed lines indicate C–H···Cl hydrogen bonds (see Figure 1), the dotted lines indicate the shortest S···S interactions which give rise to the magnetic chains running along *c*.

give rise to a chainlike motif between the radical species. However, the temperature dependence of the magnetic susceptibility (Figure 6) cannot be fitted within the regular magnetic chain model of Bonner–Fisher[24] unless a weak alternation is introduced along the chain[25] with $|J|/k = 135$ K and $\alpha = 0.95$. ($\alpha = J_1/J_2$ with $0 < \alpha < 1$). This reflects a slight dimerization of the chains upon cooling.

The strength of the C–H···Hal pincer motif was evaluated further by using a much larger halide anion, that is, the molybdenum $[Mo_6Cl_{14}]^{2-}$ cluster.[26] The electrocrystallization of **1** in the presence of $[n\text{Bu}_4\text{N}]_2[Mo_6Cl_{14}]$[27] gives rise to a 2:1 salt that incorporates acetonitrile molecules and is formulated as [**1**]$_2^{\bullet+}[Mo_6Cl_{14}]^{2-}\cdot(CH_3CN)_2$. Figure 7 shows that two organic radical cations in boat conformation surround the larger anion with a similar set of C–H···Cl hydrogen bonds, whose geometrical characteristics are collected in Table 2. This again demonstrates the efficiency of these interactions in the specific recognition of the halogenated anion. A notable

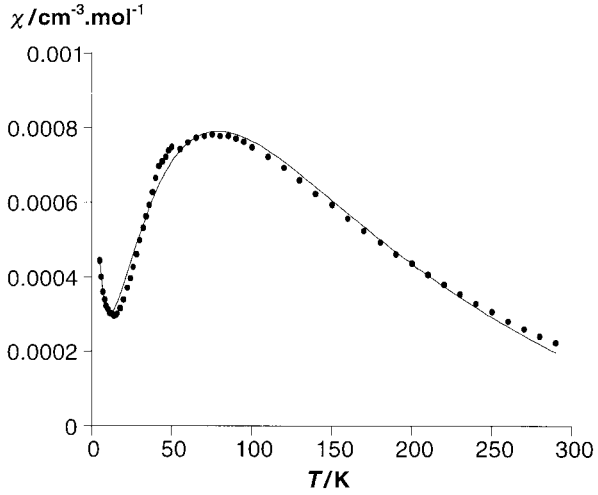

Figure 6. The temperature dependence of the magnetic susceptibility of [**1**][ICl_2]. The solid line is a fit to the alternated chain model in which $\alpha = 0.95$ and a Curie tail at low temperature encompasses 0.7 % $S = 1/2$ isolated magnetic defects.

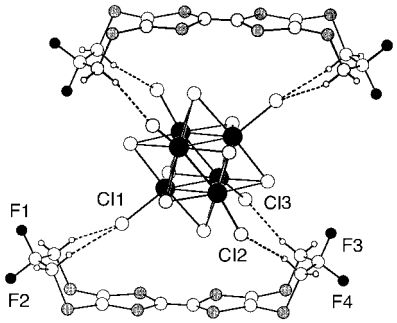

Figure 7. The trimolecular complex formed on the association of two $\mathbf{1}^{\bullet+}$ ions and $[Mo_6Cl_{14}]^{2-}$. C–H···Cl hydrogen bonds are indicated as dashed lines (see Table 2).

Table 2. Geometrical characteristics of the C–H···Hal (Hal = Cl, Br) hydrogen bonds in the $[Mo_6Cl_{14}]^{2-}$ salts of **1** and **5**.

Salt	H···Hal [Å]	C···Hal [Å]	C–H···Hal [°]
[**1**]$_2$[Mo_6Cl_{14}]	2.68 (H11B···Cl1^{i})[a]	3.562(7)	152
	2.69 (H6B···Cl2^{ii})[b]	3.578(7)	153
	2.80 (H9A···Cl1^{i})[a]	3.654(7)	148
	2.96 (H4A···Cl3^{ii})[b]	3.671(6)	131
[**5**]$_2$[Mo_6Cl_{14}]·(CH_3CN)$_2$	2.83 (H10B···Cl2^{iii})[c]	3.591(6)	136
	2.87 (H5A···Cl6^{iv})[d]	3.817(6)	165

[a] Symmetry operation i: $x, -1 + y, z$. [b] Symmetry operation ii: $-x, -1-y, -z$. [c] Symmetry operation iii: $1-x, -1/2 + y, 1/2-z$. [d] Symmetry operation iv: $x, 3/2-y, -1/2 + z$.

difference from the above structures is found in the solid-state arrangement of the supramolecular units, shown in Figure 8, which interact strongly with each other through the overlap interaction of the open-shell radical cations. This is reflected in the short interplanar distance between the two TTF cores (3.339(1) Å), in the almost eclipsed conformation, in the large HOMO···HOMO intermolecular overlap that leads to a large $\beta_{HOMO\cdots HOMO}$ interaction energy[28] (1.15 eV), and in the diamagnetic character of the salt. (The formally unpaired electrons of the two radical cations are paired in the low-lying

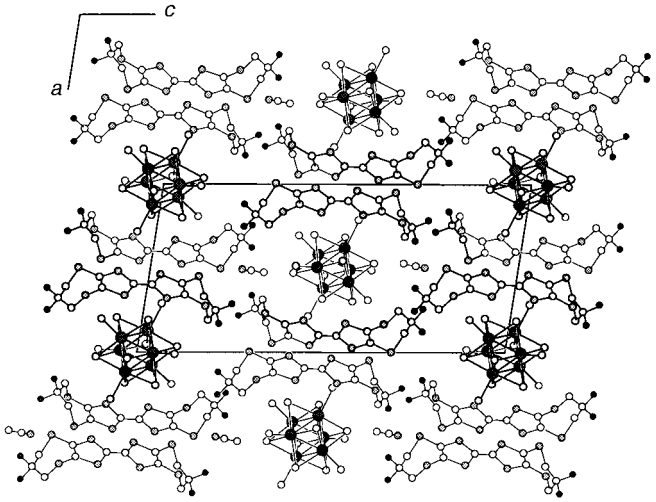

Figure 8. A projection view along the *b* axis of the unit cell of [**1**]$_2$[Mo_6Cl_{14}] which illustrates the face–face dimerization of the cation radicals, the hybrid organic/inorganic chains running along *a*, and the segregation of the fluorine atoms (shown in dark grey) and the nearby CH_3CN molecules.

bonding combination of the two individual SOMOs.) The association of the hydrogen-bonded $[\mathbf{1}]^{\bullet+}[Mo_6Cl_{14}]^{2-}[\mathbf{1}]^{\bullet+}$ trimolecular complex through the strong HOMO···HOMO overlap gives rise to hybrid organic/inorganic chains that run along the *a* axis (Figure 8). It is only the relative arrangement of those $\cdots[\mathbf{1}]_2^{2+}[Mo_6Cl_{14}]^{2-}\cdots$ chains which is then controlled by the segregation of the fluorine atoms into planes at $z = ¼$ and $z = ¾$. This segregation constraint leads to the formation of holes in the structure, which are filled by the CH_3CN solvent molecules.

A comparison with the nonfluorinated analogues: In order to evaluate the exact role played by the introduction of the fluorine atoms, the corresponding salts of the nonfluorinated bis(propylenedithio)tetrathiafulvalene (**5**) with trihalides and

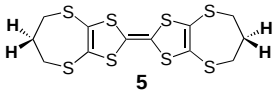

5

$[Mo_6Cl_{14}]^{2-}$ ions were investigated. While **5** has been described as affording a 2:1 phase with ICl_2^-,[29] the $[Mo_6Cl_{14}]^{2-}$ salt was unknown, and its preparation is described here. Complex [**5**]$_2$[ICl_2] was described as adopting the δ-type structure found in two-dimensional organic conductors, with alternating organic slabs of donor molecules in the chair conformation separated by inorganic ICl_2^- planes (Figure 9). The methylenic end-groups of **5** are specifically engaged, on each side, in C–H···Cl interactions with the ICl_2^- ions at the organic/inorganic interface. This arrangement is typical of most layered BEDT-TTF salts in which the ethylenic end-groups point towards the inorganic anion layers.[4] The peculiar solid-state organization of $[\mathbf{1}]^{\bullet+}[X]^-$, ($X^- = ICl_2^-$, IBr_2^-, I_2Br^-) and its similarity to **4**, in which a sulfur atom is substituted for the CF_2 group, confirms that the usual organic/inorganic segregation that prevails in conducting cation radical salts based on BEDT-TTF or BPDT-TTF (**5**) is

  0947-6539/01/0712-2638 $ 17.50+.50/0 *Chem. Eur. J.* **2001**, *7*, No. 12

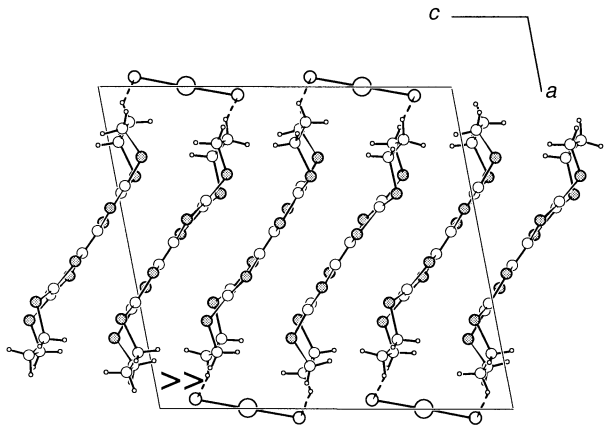

Figure 9. A projection view of the unit cell of $[\mathbf{5}]_2[ICl_2]$ with the nonfluorinated molecule **5**[29] which illustrates the typical organic/inorganic segregation and the C–H···Cl hydrogen bonds at the organic/inorganic interface (shown as dashed lines).

strongly stabilized by these C–H···Hal hydrogen bonds.[4] Suppressing these interactions by the introduction of a sulfur atom (in **4**) or a CF_2 group (in **1**) on the extremities of the donor molecules therefore has a two-fold effect: i) it destabilizes this organic/inorganic interface and prevents the formation of an organic conducting layer and ii) it activates the neighboring CH_2 groups for hydrogen bonding and stabilizes cation/anion pairs.[30]

On the other hand, $[\mathbf{5}]_2[Mo_6Cl_{14}]$ adopts a structure (Figure 10) that looks similar to its fluorinated analogue $[\mathbf{1}]_2[Mo_6Cl_{14}]\cdot(CH_3CN)_2$. The radical cations also associate into strongly overlapping dimers, as demonstrated by the distor-

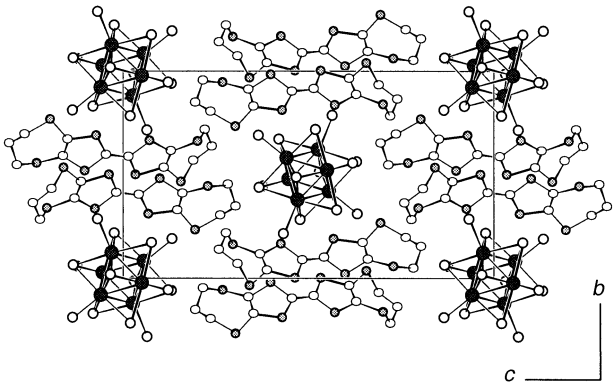

Figure 10. A projection view of the unit cell of $[\mathbf{5}]_2[Mo_6Cl_{14}]$ with the nonfluorinated molecule **5**.

tions from planarity of the TTF core, the short plane–plane distance (3.369(2) Å), the perfectly eclipsed conformation, and the strong $\beta_{HOMO\cdots HOMO}$ interaction energy (1.07 eV). Although the cationic $\mathbf{5}^{\bullet+}$ moieties are not in a boat conformation and comparable C–H···Cl interactions with the closest anion are much weaker (H···Cl > 3 Å), similar hybrid organic/inorganic $\cdots[\mathbf{5}]_2^{2+}[Mo_6Cl_{14}]^{2-}\cdots$ chains can be identified that run along the *b* axis (Figure 10). The major difference from the fluorinated analogue lies in the relative organization of these chains. They are now tightly packed together and the propylenic moieties of the $\mathbf{5}^{\bullet+}$ radical ions point toward the $[Mo_6Cl_{14}]^{2-}$ ions of the neighboring chains, while two C–H···Cl hydrogen bonds (Figure 10) are identified whose geometrical characteristics are collected in Table 2.

These two examples confirm the role of the CF_2 moieties in the fluorinated **1** in activating neighboring H atoms and in stabilization of the boat conformation of the donor molecules, which can then engage in strong organic–inorganic bimolecular or trimolecular supramolecular associations through C–H···Cl hydrogen bonds. With smaller ICl_2^-, IBr_2^-, or I_2Br^- ions, the fluorine segregation and C–H···F interactions stabilize the layered compound at the expense of the HOMO···HOMO overlap interaction. With the much larger $[Mo_6Cl_{14}]^{2-}$ ion, these segregation and hydrogen-bonding effects are probably diluted and the overlap interactions dominate the whole primary structure, which is characterized by strongly overlapping organic dimers that alternate with $[Mo_6Cl_{14}]^{2-}$ ions within hybrid organic/inorganic chains. The differences appear to be second order in the interchain interactions: i) with CF_2 segregation between chains in $[\mathbf{1}]_2[Mo_6Cl_{14}]\cdot(CH_3CN)_2$ and solvent inclusion and ii) with C–H···Cl attractive interactions between chains in $[\mathbf{5}]_2[Mo_6Cl_{14}]$ and no room left for solvent molecules. In order to recover organic/inorganic segregation and electronic conductivity in those systems, we envisioned the unsymmetrically substituted molecules **2** and **3**. While both **2** and **3** possess only one CF_2 group, the other side of the molecule includes either the ethylenic end-group of a BEDT-TTF (in **2**) or the sp^2 hydrogen atoms of a TTF donor molecule (in **3**).

Reducing the number of CF_2 groups—a route to organic/inorganic segregation: The electrocrystallization of **2** and **3** in the presence of $[n\mathrm{Bu}_4\mathrm{N}]_2[Mo_6Cl_{14}]$[27] affords two different salts of 2:1 and 4:1 stoichiometry respectively. In $[\mathbf{2}]_2[Mo_6Cl_{14}]\cdot(CH_2Cl_2)_2$ (Figure 11), strongly overlapping $[\mathbf{2}]_2^{2+}$ dimers ($\beta_{HOMO\cdots HOMO} = 1.09$ eV), which are characterized by a short plane–plane distance (3.317(2) Å), are isolated from each other by $[Mo_6Cl_{14}]^{2-}$ and exhibit only one weak C–H···Cl interaction with the closest $[Mo_6Cl_{14}]^{2-}$ ion (H···Cl: 3.019; C···Cl: 3.802(7) Å; C–H···Cl: 138.7°). The $[\mathbf{2}]^{\bullet+}[Mo_6Cl_{14}]^{2-}[\mathbf{2}]^{\bullet+}$ trimeric moieties stack into hybrid organic/inorganic chains which run along the *b* axis, as observed in **1** and **5**. The presence of a CF_2 group on the $\mathbf{2}^{\bullet+}$ radical ion limits the interchain interactions. Only one short C–H···F contact (H···F: 2.530 Å, C–H···F: 3.308(8) Å and C–H···F: 137.2°) is observed and solvent molecules (here CH_2Cl_2) are included in the voids between the chains, a situation very similar to that encountered with the fluorinated **1**.

On the other hand, $[\mathbf{3}]_4[Mo_6Cl_{14}]\cdot(CH_3CN)_2$ exhibits an extraordinary solid-state arrangement that is characterized, as shown below, by the coexistence of both the fluorine/fluorine *and* the organic/inorganic segregation together with the donor molecules in a mixed-valence state (Figure 12). Two crystallographically independent donor molecules ($\mathbf{3}_\mathbf{A}$ and $\mathbf{3}_\mathbf{B}$) are found in the unit cell together with a $[Mo_6Cl_{14}]^{2-}$ ion located on an inversion center and a CH_3CN molecule in a general position. The organic molecules are not organized into inversion-centered dimers as observed in **2**, but stack along

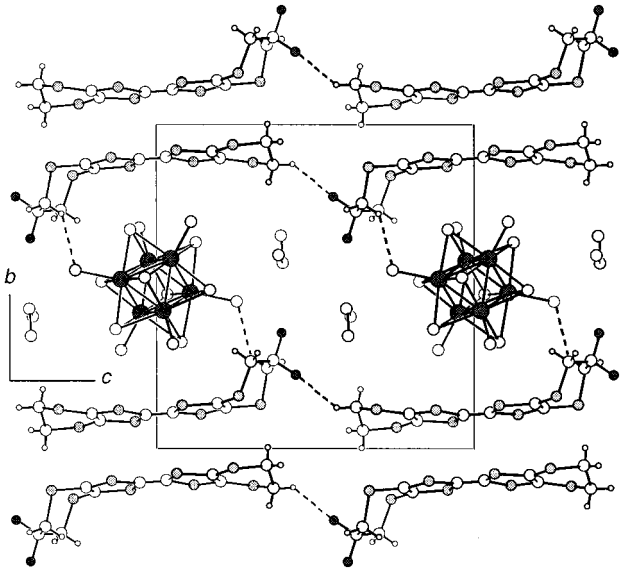

Figure 11. A projection view of the unit cell of $[\mathbf{2}]_2[Mo_6Cl_{14}]\cdot(CH_2Cl_2)_2$. The two weaker C–H···Cl and C–H···F interactions are indicated as dashed lines.

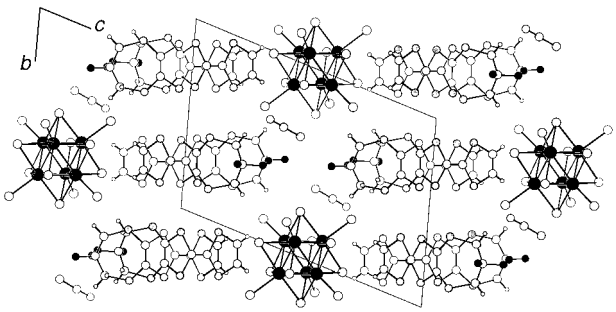

Figure 12. A projection view of the unit cell of $[\mathbf{3}]_2[Mo_6Cl_{14}]\cdot(CH_3CN)_2$ along the *a* axis which illustrates organic/inorganic segregation, the fluorine (shown in dark grey) segregation, and the C_{sp2}–H bonds of the 1,3–dithiole moieties of **3** pointing toward the chlorine atoms of the $[Mo_6Cl_{14}]^{2-}$ ion.

the *a* axis with an alternation of short (3.380(2) Å) and long (3.597(4) Å) interplanar $\mathbf{3_A}\cdots\mathbf{3_B}$ distances. The shorter one is associated with a bond-over-ring overlap, while the longer exhibits a larger longitudinal displacement. The stacks arrange parallel to each other in the *b* direction and form organic slabs. These are separated from each other by the $Mo_6Cl_{14}^{2-}$ ions and the CH_3CN molecules which fill the voids in this expanded inorganic layer. The structural arrangement is reminiscent of the 4:1 metallic phases described with BEDT-TTF and cluster anions such as the dianionic $[Mo_6Cl_{14}]^{2-}$,[26, 31, 32] $[Re_6S_6Cl_8]^{2-}$,[33] or $[Re_6Se_6Cl_8]^{2-}$.[6] Firstly, we describe the set of C–H···X hydrogen bonds before we address the overlap interaction network which develops in the organic layers. Only the unsubstituted dithiole ends of both $\mathbf{3_A}$ and $\mathbf{3_B}$ point towards the $[Mo_6Cl_{14}]^{2-}$ ion through three C_{sp2}–H···Cl interactions (Table 3); this indicates that the stabilization of organic/inorganic interfaces is not only possible with the C_{sp^3}–H hydrogen atoms of the dithioethylene fragments of BEDT–TTF, but also with C_{sp^2}–H hydrogen atoms, as observed, for example, in the TTF·chloranil complex,[34] or in EDT-TTF[35, 36] and BDT-TTP salts.[37, 38]

Table 3. C–H···X (X = Cl, N) hydrogen bond characteristics in the conducting $[\mathbf{3}]_2[Mo_6Cl_{14}]\cdot(CH_3CN)_2$ salt.

	H···X [Å]	C···X [Å]	C–H···X [°]
sp^2 C8–H8···Cl4	2.76	3.545(6)	143
sp^2 C5–H5···Cl1	2.76	3.694(6)	177
sp^3 C6–H6A···Cl3	2.78	3.596(7)	142
sp^2 C16–H16···Cl2	2.86	3.704(6)	152
sp^3 C7–H7A···Cl1	2.91	3.572(6)	126
sp^2 C17–H17···N1	2.52	3.187(7)	129
sp^3 C7–H7A···N1	2.62	3.362(7)	133
sp^3 C15–H15B···N1	2.65	3.545(7)	154

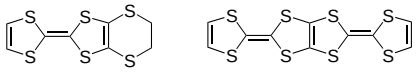

EDT-TTF BDT-TTP

We might even expect the C_{sp^2}–H hydrogen bonds to be stronger.[3] On the other side of the molecule, the CF_2 moieties face each other across the inorganic layer, while the CH_2 groups exhibit short C–H···Cl,N contacts sideways with both the $[Mo_6Cl_{14}]^{2-}$ ion and the nitrogen atom of the CH_3CN molecule (Table 2). This arrangement confirms the ambivalent character of molecule **3**, which allows the simultaneous organic/inorganic segregation, stabilization of the mixed valence species, and fluorine segregation. Within a given organic slab, the partially oxidized molecules experience a complex set of HOMO···HOMO intermolecular interactions,[28] which are shown in Figure 13. These interactions are

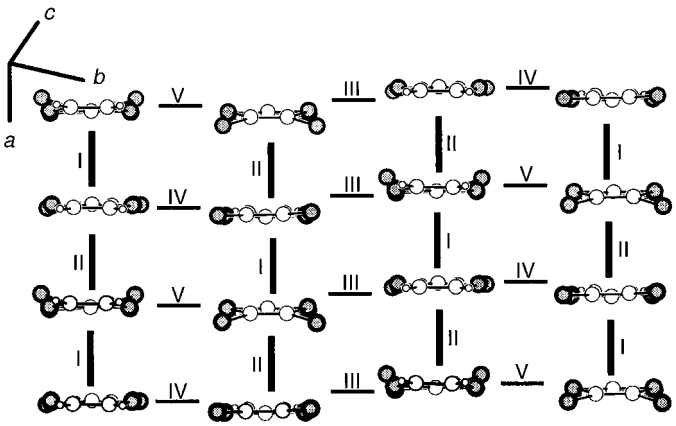

Figure 13. A view of the organic slab in $[\mathbf{3}]_2[Mo_6Cl_{14}]\cdot(CH_3CN)_2$ which shows the five different intermolecular $\beta_{HOMO\cdots HOMO}$ interactions. The calculated values of these interactions are: β_I: 0.40, β_{II}: 0.16, β_{III}: 0.10, β_{IV}: 0.16, β_V: 0.08 eV. The difluoropropylene groups have been omitted for clarity.

characterized by the formation of $\mathbf{3_A}\cdots\mathbf{3_B}$ dimers that interact with each other in the *ab* plane (interaction I). Although there are differences in detail, the layers are reminiscent, both structurally and electronically, of those in the β/β' phases of BEDT-TTF.[39]

The present layers can be described in terms of the HOMO···HOMO interactions as a series of interacting dimers in two dimensions (see the $\beta_{HOMO\text{–}HOMO}$ interaction energy values in Figure 13). The calculated band structure and

0947-6539/01/0712-2640 $ 17.50+.50/0 *Chem. Eur. J.* **2001**, *7*, No. 12

Fermi surface, which assumes a metallic filling of the bands, show (Figure 14) that the interactions along the stacks (i.e., along the *a* direction) dominate. [Note that a detailed analysis shows that the apparent lack of dispersion of the two upper bands in the $\Gamma \rightarrow Y$ direction finds its origin in an avoided crossing of the two bands.] The pseudo one-dimensional character of the Fermi surface could suggest that from the electronic viewpoint the present salt is more similar to the so-called β' salts, whose HOMO bands and the associated Fermi surface have a strong one-dimensional character,[39a] than to the so-called β salts, whose HOMO bands and the associated Fermi surface have a two-dimensional character.[4b] However,

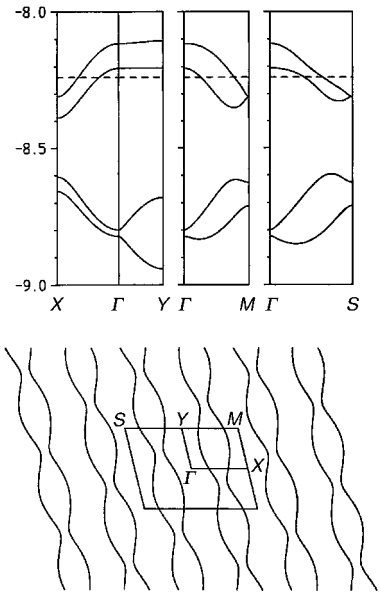

Figure 14. Band structure and Fermi surface, which assumes a metallic filling of the bands, for $[\mathbf{3}]_2[Mo_6Cl_{14}]\cdot(CH_3CN)_2$. $\Gamma = (0,0)$, $X = (a^*/2, 0)$, $Y = (0, b^*/2)$, $M = (a^*/2, b^*/2)$, and $S = (-a^*/2, b^*/2)$.

comparison of the $\beta_{HOMO-HOMO}$ interaction energies for the present salt (see Figure 13) with those typical of the β and β' salts[39] suggests that the situation here is intermediate. Since the β' salts are typically semiconducting, whereas the β salts are metallic,[4b] the observed semiconducting character of the present salt ($\sigma_{RT} = 0.02\ S\,cm^{-1}$) raises an obvious question: can the metallic regime (observed in the β phases) be attained by increasing the interaction between dimers, for example, by applying pressure? Alternatively, it will be of interest to investigate the magnetic properties of this salt since the β' phases frequently exhibit an antiferromagnetic ground state.[40] Finally, let us note that it is quite likely that the electron-withdrawing effect of the fluorine atoms has a role not only in the structural arrangement which is observed here, but also in the activated electron hopping. This withdrawing effect, which is transmitted throughout the σ-bonds, will tend to keep the formally unpaired electron in the dimeric units (as observed in the β' phases, although for stronger structural reasons that result in a much stronger alternation of HOMO···HOMO interactions along the stacks).

Conclusion

Although fluorine segregation of the CF_2 fragments is observed in the different phases described here, it is clear that the neighboring, activated CH_2 moieties play a paramount role in the structural organization. Indeed, C–H···F interactions are known to influence the structural arrangement of neutral, fluorinated molecules that incorporate activated hydrogen atoms, but the introduction of halogenated anions such as ICl_2^- or $Mo_6Cl_{14}^{2-}$ strongly favors the formation of C–H···Cl,Br,I hydrogen bonds with the more polarizable halogens. The precise position of these hydrogen atoms on the TTF core influences the structural hydrogen-bonded motifs and, indeed, the whole solid-state organization and electronic properties. In fact, as **1** incorporates two CF_2 groups on the molecular ends (and four CH_2 ones along the sides), a boat-shape conformation stabilizes the bi- or trimolecular coordination of the linear or cluster anions. With smaller anions, the fluorine segregation controls the solid-state arrangement, while larger anions allow the overlap interaction to dominate the structural organization whatever the number of CF_2 groups: comparable structures are obtained with $[Mo_6Cl_{14}]^{2-}$ and **1**, **2**, or **5**. The two-dimensional organic/inorganic segregation obtained with **3** demonstrates the sensitivity of the energetic balance. Indeed, it is recovered only when one end of the TTF core bears C_{sp^2}–H groups that are able to engage in directional C–H···Hal hydrogen bonds which are oriented parallel to the long molecular axis and toward the anionic layer; this demonstrates the role of those C–H···Hal hydrogen bonds in the stabilization of such conducting phases. Therefore, a fully perfluorinated donor molecule is not expected to crystallize in the presence of the usual anions, but possibly in the presence of fluorinated anions. This is currently under investigation.

In the salts described here, CH_3CN or CH_2Cl_2 solvent inclusion is found only in the presence of one (in **2** or **3**) or two (with **1**) CF_2 groups. This observation can be correlated to the open-framework structures described by Fujita et al.[41]; these are based on linear, bidentate, and highly fluorinated pyridyl ligands, whose $Cd(NO_3)_2$ salts crystallize with large cavities that can incorporate different aromatic solvent molecules. The weak intermolecular interactions between fluorinated molecules were shown to favor "hetero-recognition" (by enclathration) rather than "self-recognition" (by constriction or interpenetration). A similar effect is most probably at work here and underlines the rich solid-state chemistry that fluorinated molecules can offer in the elaboration of novel structures that possess specific structural and electronic properties, for example low-dimensionality, porosity, conductivity, or magnetism.

Experimental Section

Electrocrystallization experiments:[42] The starting compound (**1**–**5**, 6 mg) was oxidized in the presence of the tetra-*n*-butyl ammonium salt of the desired counter anion (100 mg) in freshly distilled CH_3CN (12 mL). The electrocrystallization was carried out in two-compartment cells with platinum electrodes ($l = 2$ cm, $\varnothing = 1$ mm) at a constant current (0.5–2 μA) at 20 °C.

Data collection and structure determination: Table 4 summarizes the details of crystallographic data collection and structure refinement. Data were collected at room temperature on an Imaging Plate Diffraction System (Stoe – IPDS). Structures were solved by direct methods by using SHELXS-86 and refined by the full-matrix least-squares method on F^2, by using SHELXL-93 (G. M. Sheldrick, University of Göttingen, 1993). Anisotropic thermal parameters were used for all non-hydrogen atoms. The hydrogen atoms were introduced at calculated positions (riding model) with C_{sp^2}–H and C_{sp^3}–H bond lengths of 0.93 and 0.97 Å, respectively. Crystallographic data (excluding structure factors) for the structures reported in this paper have been deposited with the Cambridge Crystallographic Data Centre as supplementary publication no. CCDC-151754 to CCDC—151760. Copies of the data can be obtained free of charge on application to CCDC, 12 Union Road, Cambridge CB2 1EZ, UK (fax: (+44) 1223-336-033; e-mail: deposit@ccdc.cam.ac.uk).

Band structure calculations: The band structure calculations[43] were of the extended Hückel type.[44] A modified Wolfsberg – Helmholtz formula was used to calculate the non-diagonal $H_{\mu\nu}$ values.[45] Double-ζ orbitals for C, F, and S were used.[46]

Magnetic measurements: Magnetic susceptibility measurements were performed on a Quantum Design MPMS – 2 SQUID magnetometer operating on the range 4 – 300 K at 25000 G with polycrystalline samples of [**1**][ICl_2]. Data were corrected for sample holder contribution and Pascal diamagnetism.

Acknowledgements

We thank Pascale Auban-Senzier (Laboratoire de Physique des Solides, Orsay, France) for conductivity measurements. Financial support from the CNRS and the Région Pays de Loire (to O.J.D.), DGES (Spain—Project PB96-0859) and Generalitat de Catalunya (1999 SGR 207) (to E.C.) is gratefully acknowledged.

[1] a) J. Riess, *New. J. Chem*. **1995**, *19*, 891; b) J. Höpken, M. Möller, *Macromolecules* **1992**, *25*, 2482; c) F. Guitard, E. Taffin de Givenchy, S. Geribaldi, A. Cambon, *J. Fluorine Chem*. **1999**, *100*, 85.
[2] O. J. Dautel, M. Fourmigué, *J. Org. Chem.* **2000**, *65*, 6479.
[3] For weak C–H ··· X hydrogen bonds, see: G. R. Desiraju, T. Steiner, in *The Weak Hydrogen Bond*, Oxford University Press, Oxford, **1999**.
[4] a) M.-H. Whangbo, *Acc. Chem. Res.* **1983**, *16*, 95; b) J. M. Williams, J. R. Ferraro, R. J. Thorn, K. D. Carlson, U. Geiser, H. H. Wang, A. M. Kini, M.-H. Whangbo, in *Organic Superconductors (Including Fullerenes)*, Prentice Hall, Engelwood Cliffs, NJ, **1992**.
[5] a) M.-H. Whangbo, J. M. Williams, A. J. Schultz, T. J. Emge, M. A. Beno, *J. Am. Chem. Soc.* **1987**, *109*, 90; b) M.-H. Whangbo, D. Jung, J. Ren, M. Evain, J. J. Novoa, F. Mota, S. Alvarez, J. M. Williams, M. A. Beno, M. A. Kini, H. H. Wang, J. R. Ferraro, in *The Physics and Chemistry of Organic Superconductors* (Eds.: G. Saito, S. Kagoshima), Springer, Heidelberg, Germany, **1990**, 262; c) A. Davidson, K. Boubekeur, A. Pénicaud, P. Auban, C. Lenoir, P. Batail, G. Hervé, *J. Chem. Soc. Chem. Commun*. **1989**, 1373; d) A. Deluzet, P. Batail, Y. Misaki, P. Auban-Senzier, E. Canadell, *Adv. Mater*. **2000**, *12*, 436.
[6] A. Pénicaud, K. Boubekeur, P. Batail, E. Canadell, P. Auban – Senzier, D. Jérome, *J. Am. Chem. Soc*. **1993**, *115*, 4101.
[7] a) J. A. Schlueter, J. M. Williams, U. Geiser, J. D. Dudek, M. E. Kelly, S. A Sirchio, K. D. Carlson, D. Naumann, T. Roy, C. F. Campana, *Adv. Mater*. **1995**, *7*, 634; b) B. H. Ward, J. A. Schlueter, U. Geiser, H. H. Wang, E. Morales, J. P. Parakka, S. Y. Thomas, J. M. Willams, P. G. Nixon, R. W. Winter, G. L. Gard, H.-J. Koo, M.-H. Whangbo, *Chem. Mater.* **2000**, *12*, 343.
[8] G. R. Desiraju, *Angew. Chem.* **1995**, *107*, 2505; *Angew. Chem. Int. Ed. Engl*. **1995**, *34*, 2371.
[9] a) K. Heuzé, C. Mézière, M. Fourmigué, P. Batail, C. Coulon, E. Canadell, P. Auban-Senzier, D. Jérome, *Chem. Mater*. **2000**, *12*, 1898; b) K. Heuzé, M. Fourmigué, P. Batail, E. Canadell, P. Auban-Senzier, *Chem. Eur. J.* **1999**, *5*, 2971; c) M. R. Bryce, *J. Mater. Chem*. **1995**, *5*, 1481.
[10] a) A. Dolbecq, A. Guirauden, M. Fourmigué, K. Boubekeur, P. Batail, M.-M. Rohmer, M. Bénard, C. Coulon, M. Sallé, P. Blanchard, *J. Chem. Soc. Dalton Trans.* **1999**, 1241; b) A. Dolbecq, M. Fourmigué,

Table 4. Crystallographic data.

	[**1**][ICl_2]	[**1**][IBr_2]	[**1**][I_2Br]	[**1**]$_2$[Mo_6Cl_{14}] · $(CH_3CN)_2$	[**5**]$_2$[Mo_6Cl_{14}]	[**2**]$_2$[Mo_6Cl_{14}] · $(CH_2Cl_2)_2$	[**3**]$_2$[Mo_6Cl_{14}] · $(CH_3CN)_2$
formula	$C_{12}H_8F_4S_8ICl_2$	$C_{12}H_8F_4S_8IBr_2$	$C_{12}H_8F_4S_8I_{1.5}Br_{1.5}$	$C_{28}H_{22}Cl_{14}F_8Mo_6N_2S_{16}$	$C_{24}H_{24}S_{16}Mo_6Cl_{14}$	$C_{24}H_{20}Cl_{18}F_4Mo_6S_{16}$	$C_{40}H_{30}Cl_{14}F_8Mo_6N_2S_{24}$
M_W	682.46	771.38	794.88	2123.38	1897.33	2111.10	2532.04
color/habit	black/plates	black/plates	black/plates	black/plates	black/needles	black/parallograms	black/needles
size [mm]	0.12 × 0.10 × 0.023	0.2 × 0.2 × 0.025	0.2 × 0.12 × 0.03	0.46 × 0.11 × 0.04	0.23 × 0.10 × 0.08	0.20 × 0.14 × 0.13	0.38 × 016 × 016
crystal system	orthorhombic	orthorhombic	orthorhombic	monoclinic	monoclinic	monoclinic	triclinic
space group	$Cmc2_1$	$Cmc2_1$	$Cmc2_1$	$P2_1/n$	$P2_1/c$	$P2_1/n$	$P\bar{1}$
a [Å]	28.816(2)	28.813(6)	28.812(2)	12.664(3)	10.008(2)	12.948(3)	9.4427(19)
b [Å]	8.6985(7)	8.776(2)	8.8070(9)	9.2764(19)	12.309(3)	15.594(3)	12.985(3)
c [Å]	8.5007(6)	8.553(2)	8.5720(9)	27.090(5)	22.197(4)	15.500(3)	17.241(3)
α [°]	–	–	–	–	–	–	71.55(3)
β [°]	–	–	–	98.81(3)	97.35(3)	100.61(3)	85.58(3)
γ [°]	–	–	–	–	–	–	76.31(3)
V [Å^3]	2130.8(3)	2162.8(3)	2175.1(3)	3144.9(11)	2712.1(9)	3076.2(11)	1948.3(7)
Z	4	4	4	2	2	2	1
ρ_{calcd} [g cm^{-3}]	2.127	2.369	2.427	2.242	2.323	2.279	2.158
μ [mm^{-1}]	2.570	5.980	5.738	2.340	2.677	2.549	2.114
θ range [°]	2.45 – 25.84	2.43 – 25.80	2.42 – 25.84	1.65 – 26.05	1.65 – 26.05	1.65 – 26.05	1.65 – 26.05
h,k,l index ranges	±35, ±10, ±10	±35, ±10, ±10	±35, ±10, ±10	±15, ±11, ±33	±12, ±15, ±27	±15, ±18, ±19	±11, ±15, ±21
reflections collected	6078	5461	6390	24482	21034	23893	18824
absorption correction	numerical	numerical	numerical	empirical	numerical	numerical	numerical
T_{min}/T_{max}	0.7752/0.9321	0.3437/0.8801	0.4929/0.8600	0.6282/0.9182	0.7222/0.8230	0.6481/0.8507	0.5801/0.7615
independent reflections	2097	1996	2090	5861	5042	5705	6954
R_{int}	0.0689	0.0587	0.116	0.043	0.110	0.048	0.0409
observed reflections	1478	1395	1239	4273	2697	3789	5411
parameters	124	124	124	334	271	302	409
$R1$[a]	0.0365	0.038	0.0472	0.0266	0.0381	0.0302	0.0271
$wR2$[b]	0.0513	0.0727	0.1049	0.0534	0.0557	0.0613	0.0668
GOF[c]	0.852	1.006	0.814	0.889	0.766	0.828	0.931
$\Delta\rho_{max/min}$ [e^{-3}]	0.69/ – 0.61	0.88/ – 0.46	0.88/ – 0.67	0.44/ – 0.50	0.93/ – 0.70	0.82/ – 0.79	0.93/ – 0.39

[a] $R1 = \Sigma(||F_o;| - |F_c||)/\Sigma|F_o|$. [b] $wR2 = [\Sigma w(F_o^2 - F_c^2)^2/\Sigma w(F_o^2)^2]^{1/2}$. [c] $GOF = [w(F_o^2 - F_c^2)^2/(NO - NV)]^{1/2}$.

F. C. Krebs, P. Batail, E. Canadell, R. Clérac, C. Coulon, *Chem. Eur. J.* **1996**, *2*, 1275; c) A. Dolbecq, M. Fourmigué, P. Batail, C. Coulon, *Chem. Mater*. **1994**, *6*, 1413.

[11] a) G. R. Desiraju, R. Parthasarasthy, *J. Am. Chem. Soc.* **1989**, *111*, 8725; b) S. L. Price, A. J. Stone, J. Lucas, R. S. Rowland, A. E. Thornley, *J. Am. Chem. Soc*. **1994**, *116*, 4910.

[12] a) Y. Kuwatani, E. Ogura, H. Nishkawa, I. Ikemoto, M. Iyoda, *Chem. Lett*. **1997**, 817; b) M. Iyoda, H. Suzuki, S. Sasaki, H. Yoshino, K. Kikuchi, K. Saito, I. Ikemoto, H. Matsuyama, T. Mori, *J. Mater. Chem.* **1996**, *6*, 501.

[13] a) T. Imakubo, H. Sawa, R. Kato, *Synth. Met.* **1995**, *73*, 117; b) T. Imakubo, H. Sawa, R. Kato, *J. Chem. Soc. Chem. Commun.* **1995**, 1667; c) T. Imakubo, T. Maruyama, H. Sawa, K. Kobayashi, *Chem. Commun*. **1998**, 2021.

[14] a) G. R. Desiraju, R. L. Harlow, *J. Am. Chem. Soc.* **1989**, *111*, 6757; b) J. P. M. Lommerse, A. J. Stone, R. Taylor, F. H. Allen, *J. Am. Chem. Soc*. **1996**, *118*, 3108.

[15] A. C. Legon, *Angew. Chem.* **1999**, *111*, 2850; *Angew. Chem. Int. Ed.* **1999**, *38*, 2687.

[16] E. Laukhina, J Vidal-Gancedo, S. Khasanov, V. Tkacheva, L. Zorina, R. Shibaeva, J. Singelton, R. Wojciechowski, J. Ulanski, V. Laukhin, J. Veciana, C. Rovira, *Adv. Mater.* **2000**, *12*, 1205.

[17] a) T. Steiner, *Acta Crystallogr. Sect. B* **1998**, *54*, 456; b) C. B. Aakerôy, T. A. Evans, K. R. Seddon, I. Palinko, *New J. Chem*. **1999**, 145.

[18] M. Freytag, P. G. Jones, *Chem. Commun*. **2000**, 277.

[19] J. D. Dunitz, R. Taylor, *Chem. Eur. J.* **1997**, *3*, 89.

[20] J. A. K. Howard, V. J. Hoy, D. O'Hagan, G. Smith, *Tetrahedron* **1996**, *52*, 12 613.

[21] V. R. Thalladi, H.-C. Weiss, D. Bläser, R. Boese, A. Nangia, G. R. Desiraju, *J. Am. Chem. Soc.* **1998**, *120*, 8702.

[22] a) C. Dai, P. Nguyen, T. B. Marder, A. J. Scott, W. Clegg, C. Viney, *Chem. Commun*. **1999**, 2493; b) J. W. Bats, J. Parsch, J. W. Engels, *Acta Crystallogr. Sect. C* **2000**, *56*, 201.

[23] V. E. Korotkov, R. P. Shibaeva, *Kristallografiya* **1991**, *36*, 1139.

[24] J. C. Bonner, M. E. Fisher, *Phys. Rev. A* **1964**, 640.

[25] a) O. Kahn, in *Molecular Magnetism*, VCH, New York, 1993; b) J. W. Hall, W. E. Marsh, R. R. Weller, W. E. Hatfield, *Inorg. Chem*. **1981**, *20*, 1033.

[26] a) E. Amberger, H. Fuchs, S. Fuchs, K. Polborn, T. Lehnert, *Synth. Met.* **1987**, *19*, 605; b) P. Batail, C. Livage, S. S. P. Parkin, C. Coulon, J. D. Martin, E. Canadell, *Angew. Chem.* **1991**, *103*, 1508; *Angew. Chem. Int. Ed. Engl.* **1991**, *30*, 1498.

[27] P. Nanelli, B. P. Block, *Inorg. Synth*. **1970**, *12*, 170.

[28] M.-H. Whangbo, J. M. Williams, P. C. W. Leung, M. A. Beno, T. J. Emge, H. H. Wang, *Inorg. Chem*. **1985**, *24*, 3500.

[29] a) J. M. Williams, T. J. Emge, M. A. Firestone, H. H. Wang, M. A. Beno, U. Geiser, L. Numez, K. D. Carlson, *Mol. Cryst. Liq. Cryst*. **1987**, *148*, 233; b) R. P. Shibaeva, L. P. Rozenberg, M. A. Simonov, N. D. Kushch, E. B. Yagubski, *Kristallografiya* **1988**, *33*, 1156.

[30] A similar destabilization of the organic/inorganic interface is probably at work also in the salts of the S-position isomers of BEDT–TTF in which the CH_2 and S groups of BEDT–TTF have been inverted: P. Hudhomme, P. Blanchard, M. Sallé, S. Le Moustarder, A. Riou, M. Jubault, A. Gorgues, G. Duguay, *Angew. Chem.* **1997**, *109*, 896; *Angew. Chem. Int. Ed. Engl.* **1997**, *36*, 878.

[31] H. Fuchs, S. Fuchs, K. Polborn, T. Lehnert, C. P. Heidmann, H. Müller, *Synth. Met.* **1988**, *27*, 271.

[32] C. J. Kepert, M. Kurmoo, P. Day, *Proc. R. Soc. London A* **1998**, *454*, 487.

[33] a) A. Deluzet, Ph.D. Thesis, Nantes (France), **2000**; b) C. Guilbaud, PhD. Thesis, Nantes (France), **1998**.

[34] P. Batail, S. J. LaPlaca, J. J. Mayerle, J. B. Torrance, *J. Am. Chem. Soc.* **1981**, *103*, 951.

[35] a) A. Terzis, A. Hountas, G. C. Papavassiliou, B. Hilti, J. Pfeiffer, *Acta Crystallogr. Sect. C* **1990**, *46*, 224; b) A. Hountas, A. Terzis, G. C. Papavassiliou, B. Hilti, M. Bürckle, C. W. Mayer, J. Zambounis, *Acta Crystallogr. Sect. C* **1990**, *46*, 228; c) R. Kato, H. Kobayashi, A. Kobayashi, *Chem. Lett*. **1989**, 781.

[36] K. Boubekeur, R. Riccardi, P. Batail, E. Canadell, *C. R. Acad. Sci. Ser. IIc* **1998**, 627.

[37] a) Y. Misaki, T. Matsui, K. Kawakami, H. Mishikawa, T. Yamabe, M. Shiro, *Chem. Lett*. **1993**, 1337; b) T. Mori, Y. Misaki, H. Fujiwara, T. Yamabe, *Bull. Chem. Soc. Jpn*. **1994**, *67*, 2685; c) Y. Misaki, H. Fujiwara, T. Yamabe, T. Mori, H. Mori, *Chem. Lett*. **1994**, 1653.

[38] a) Y. Misaki, T. Miura, M. Taniguchi, H. Fujiwara, T. Yamabe, T. Mori, H. Mori, S. Tanaka, *Adv. Mater*. **1999**, *9*, 714; b) A. Deluzet, P. Batail, Y. Misaki, P. Auban-Senzier, E. Canadell, *Adv. Mater.* **2000**, *12*, 436.

[39] a) T. J. Emge, H. H. Wang, P. C. W. Leung, P. R. Rust, J. D. Cook, P. L. Jackson, K. D. Carlson, J. M. Williams, M.-H. Whangbo, E. L. Venturini, J. F. Schriber, L. J. Azevedo, J. R. Ferraro, *J. Am. Chem. Soc*. **1986**, *108*, 695; b) T. Mori, *Bull. Chem. Soc. Jpn*. **1998**, *71*, 2509.

[40] a) C. Coulon, R. Laversanne, J. Amiell, P. Delhaes, *J. Phys. C Solid State Phys.* **1986**, *19*, L753; b) T. J. Emge, H. H. Wang, M. K. Bowman, C. M. Pipan, K. D. Carlson, M. A. Beno, L. N. Hall, B. A. Anderson, J. M. Williams, M.-H. Whangbo, *J. Am. Chem. Soc*. **1987**, *109*, 2016.

[41] a) K. Kasai, M. Aoyagi, M. Fujita, *J. Am. Chem. Soc.* **2000**, *122*, 2140; b) M. Fujita, S. Nagao, M. Iida, K. Ogata, K. Ogura, *J. Am. Chem. Soc*. **1993**, *115*, 1574.

[42] For a general reference on the technique, see: P. Batail, K. Boubekeur, M. Fourmigué, J.-C. P. Gabriel, *Chem. Mater*. **1998**, *10*, 3005.

[43] M.-H. Whangbo, R. Hoffmann, *J. Am. Chem. Soc*. **1978**, *100*, 6093.

[44] R. Hoffmann, *J. Chem. Phys.* **1963**, *39*, 1397.

[45] J. H. Ammeter, H.-B. Bürgi, J. Thibeault, R. Hoffmann, *J. Am. Chem. Soc.* **1978**, *100*, 3686.

[46] E. Clementi, C. Roetti, *At. Data Nucl. Data Tables* **1974**, *14*, 177.

Received: November 24, 2000 [F2896]